07-CO80
LA-UR-~~06~~-

Approved for public release; distribution is unlimited.

Title: MCNP/X Transport in the Tabular Regime

Author(s): H. Grady Hughes

Intended for: Proceedings of the Hadronic Shower Simulation Workshop
Fermi National Accelerator Laboratory
Batavia, Illinois
6-8 September 2006

Los Alamos
NATIONAL LABORATORY
EST. 1943

Los Alamos National Laboratory, an affirmative action/equal opportunity employer, is operated by the Los Alamos National Security, LLC for the National Nuclear Security Administration of the U.S. Department of Energy under contract DE-AC52-06NA25396. By acceptance of this article, the publisher recognizes that the U.S. Government retains a nonexclusive, royalty-free license to publish or reproduce the published form of this contribution, or to allow others to do so, for U.S. Government purposes. Los Alamos National Laboratory requests that the publisher identify this article as work performed under the auspices of the U.S. Department of Energy. Los Alamos National Laboratory strongly supports academic freedom and a researcher's right to publish; as an institution, however, the Laboratory does not endorse the viewpoint of a publication or guarantee its technical correctness.

Form 836 (7/06)

MCNP/X Transport in the Tabular Regime

H. Grady Hughes

Los Alamos National Laboratory
Group X-3-MCC, MS A143
Los Alamos, NM 87545 USA

Abstract. We review the transport capabilities of the MCNP and MCNPX Monte Carlo codes in the energy regimes in which tabular transport data are available. Giving special attention to neutron tables, we emphasize the measures taken to improve the treatment of a variety of difficult aspects of the transport problem, including unresolved resonances, thermal issues, and the availability of suitable cross sections sets. We also briefly touch on the current situation in regard to photon, electron, and proton transport tables.

Keywords: Monte Carlo; neutron transport; particle transport; nuclear data tables.
PACS: 28.20.Gd

INTRODUCTION

Traditionally, and quite understandably, high-energy particle transport codes have enjoyed less extensive development for the low-energy regime than for high-energy processes. However, many aspects of low-energy transport are important for high-energy facilities and experiments. For example, the low-energy background of an experiment can significantly impact its interpretation. Similarly, the proper characterization of low-energy contributions to calorimeters can be essential, as is discussed elsewhere in this meeting. Serious personnel safety issues in facility shielding design also mandate a full understanding of the transport cascade, including the effects of low-energy particles. Some high-energy facilities (spallation sources) exist entirely for the purpose of producing low-energy secondary particles, such as neutrons for materials science research, production of useful isotopes, etc. Environmental issues, such as air and groundwater activation, are also related to low-energy particle behavior. For these and other reasons, the developers of high-energy transport codes are putting increasing efforts into improving their modeling of transport in the low-energy regime.

In contrast to most high-energy codes, MCNP[1] began life as a low-energy code transporting neutrons and photons (and later electrons) in energy ranges typically below 20 MeV. Important applications included reactor design, criticality safety, radiation shielding and protection, and later electron accelerator design, medical physics, and many other aspects of the low-energy world. Before high-energy transport methods and an extended set of particle types were introduced, first in the MCNPX code[2] and later in the (not yet released) developmental version[3] of MCNP itself, low-energy capabilities benefited from the full attention of the MCNP developers. As a result, the MCNP/X codes are a uniquely valuable resource especially for high-energy applications in which the low-energy component is important. In this paper we shall review a number of the specific capabilities of the MCNP/X codes in the low-energy regime, with particular attention to those aspects that are associated with use of nuclear data tables.

EVALUATED NUCLEAR DATA TABLES

The essential source of the transport physics for MCNP is the collection of evaluated nuclear data tables that are developed and distributed with the code. MCNP uses data tables in a format based on the Evaluated Nuclear Data File[4] (ENDF), a national (and by now international) standard for format and content established and monitored by the Cross Section Evaluation Working Group (CSEWG). The ENDF tables can be supplemented by other evaluated sets such as the Evaluated Nuclear Data Library[5] (ENDL), leading to a powerful and quite general compilation of data for use in transport calculations. For example, a recent release of cross-section data for MCNP includes 974 "continuous energy" neutron tables covering 250 isotopes among 80 elements ranging from Z=1 to Z=98.

There are a number of different kinds of tables represented in the collection of transport data distributed with the code. We have mentioned "continuous energy" neutron tables, which constitute the most detailed available description of neutron transport. These tables typically address neutron processes from very low energies (on the order of 10^{-5} eV) up to the MeV range. Older tables, driven by applications such as reactor design or radiation shielding, often ended at 20 MeV. More recent ENDF releases, motivated by applications to be addressed by the MCNPX code, continue to 150 MeV. We shall discuss the contents of continuous-energy neutron tables in the next section, and the supplementary $S(\alpha,\beta)$ thermal tables in a later section.

Besides continuous-energy data, MCNP can use multigroup tables familiar from deterministic methods. This kind of data table represents the cross sections as averages over energy groups weighted by assumed energy-flux spectra. The energy groups are generally much larger than the resolution of continuous-energy tables, so that much detail is lost, especially in the neutron resonance region. For example, Figure 1 shows the total cross section for naturally occurring iron over most of the energy range of the ENDF/B-V evaluation, contrasting the detailed presentation of the continuous-energy table (26000.55c) with the relatively crude representation of a typical multigroup table (26000.55m). Further, the dependence on the assumed energy spectrum makes the results quite problem-dependent and requires a great deal of insight in the selection or preparation of the cross sections. For a wide range of Monte Carlo applications, there is now little reason to prefer a multigroup approach. However, there are special circumstances in which multigroup transport offers considerable advantage. For example, in simulations featuring diffuse, extended sources and very localized detectors (tallies), the adjoint method will usually provide a more efficient calculation than the standard forward method. Adjoint Monte Carlo in MCNP is only available as multigroup transport and requires the use of multigroup cross sections. Another popular method requiring multigroup tables is the simulation of coupled electron/photon transport by the Boltzmann-Fokker-Planck[6] (BFP) algorithm. Here the electrons and photon masquerade as neutrons and appropriate multigroup tables can be generated with the CEPXS[7] code developed by Sandia National Laboratory. Another area of recent interest is the use of a deterministic method to pre-calculate phase-space importances or weight-window parameters for variance reduction in a forward Monte Carlo calculation. In this hybrid method, the multigroup cross sections for the deterministic calculation correspond as closely as possible to the continuous-energy cross sections of the eventual Monte Carlo calculation. Finally, multigroup calculations may be needed in the context of validation and verification to compare Monte Carlo results with those of deterministic transport methods, in scoping studies or sensitivity studies, or to simulate isotopes for which continuous-energy cross sections are unavailable.

FIGURE 1 place holder

FIGURE 1. Total cross section for naturally-occurring iron from ENDF/B-V (26000.55c) and from an ENDF/B-V-based multigroup tabulation (26000.55m).

The data libraries distributed with MCNP also include an extensive set of neutron dosimetry cross sections. These tables are not full transport tables in the sense of the next section, and cannot be used to model the neutron transport in the specified isotope. Rather they contain energy-dependent cross sections for various specific reactions that neutrons may induce in the particular isotope. Thus these tables are suitable for calculation of reaction rates for trace elements in an experiment by integrating the reaction cross sections weighted by the neutron energy-flux spectrum. This capability is frequently used in neutron dosimetry and neutron activation applications. To generate these data, ENDF sources (ENDF/B-V Dosimetry Tape 531 and Activation Tape 532) are supplemented with ACTL[8], an evaluated neutron activation cross-section library from Lawrence Livermore National Laboratory. The current MCNP distribution includes 463 isotopes of 82 elements from Z=1 to Z=98.

CONTENTS OF CONTINUOUS-ENERGY NEUTRON TABLES

Continuous-energy cross sections are not, of course, continuous in the mathematical sense. They are necessarily tabulations of various data at a discrete set of energies. The word "continuous" is meant to suggest that, unlike multigroup data, the tabulation is for a set of energies sufficiently dense that all of the edges, resonances, and sundry features of the physical evaluation are completely represented to within some prescribed small tolerance. With modern data, that tolerance is typically 1% or better. Many recent tables have been processed with tolerances of 0.1%. In order to provide a complete description of the physical processes, data libraries must incorporate a large amount of information. There must be a transport table available for each isotope present in a simulation. Each of these tables must provide as a function of energy a full accounting of the reactions that a neutron may undergo with the given isotope. For all energies, total, absorption, and elastic cross sections, and average heating numbers are given. For each reaction channel in the evaluation, partial cross sections and reaction-specific Q-values are provided. For every reaction producing secondary particles (other neutron, photons, or other particles types), energy and angular probability distributions for sampling must exist. There may be a large number of reaction channels. For example a recent tabulation for ^{56}Fe (26056.66c) contains individual information for (n,2n), (n,np), and (n,nα) reactions, for excitation to the first 25 excited states, and for excitation to the continuum. For fissionable isotopes, total fission cross sections and average ν (number of fission neutrons) must be present along with fission neutron energy distributions. In many cases, both ν and fission neutron spectra will be tabulated separately for prompt fission and for several modes of delayed fission together with channel probabilities.

In the generation of secondary particles, some sampling distributions are correlated in reaction channel, energy, and angle. For example, elastic scattering is microscopically correct because energy-momentum conservation can be imposed in the sampling process. Some other sampling distribution are coupled in energy and angle as well. However, many distributions for secondary particles are provided as independent energy spectra and angular distributions and therefore lead to uncorrelated sampling of the secondary-particle phase space. In addition, in any reaction generating more than one secondary particle, the various particles from the reaction will be sampled independently. The best-known example of this situation is the fact that neutron-induced photons are generated from the photon-production probability distributions without regard to the selection of the actual neutron reaction. The result of all this lack of correlation is that MCNP, using tabular neutron data, is not well suited to the simulation of coincidence experiments and other application of "microscopically correct" tallies. However, these matters are irrelevant to the macroscopic tallies of MCNP such as particle flux and current, energy spectra, angular distributions, reaction rates, energy deposition, etc. For these standard calculations of integrated quantities, the important issue is the correctness of the transport methods in the average.

UNRESOLVED RESONANCE PROBABILITY TABLES

In Figure 1 we saw an example of a cross-section table containing sufficient data to represent an essentially complete description of the transport process over the entire range of the table. By contrast consider Figure 2, which shows two different tabulations of the total cross section for ^{235}U, specifically an older set from ENDF/B-V (92235.50c) and a newer set from ENDF/B-VI (92235.69c). The abrupt loss of detail (at just above 0.08 keV for the older table and above 2.25 keV for the newer) clearly indicates that the nuclear resonance region is incompletely described in both evaluations. In fact the resonance region for ^{235}U extends up to 25 keV. The meandering curve representing the total cross section above the detailed portion of the resonance region is simply an average of the cross section over energy ranges in which full data are not available. The neglect of the details of the cross section in the unresolved-resonance region would ignore self-shielding effects, which can have a significant impact on the results of the calculation. While the application programmer should be strongly motivated to use the latest cross-section sets, with their increased coverage of the resonance region, the problem of an unresolved region remains.

Fortunately, modern evaluations provide an excellent approximation for dealing with this problem. Beginning with MCNP version 4C (and therefore MCNPX) and later versions, the code is able to take advantage[9] of cross-section probability tables derived from statistical information in evaluations such as average level spacings and average resonance widths. When these data are provided in a transport table, a probabilistic approach can be taken in which the cross section encountered by the neutron in the unresolved resonance region is sampled from a probability distribution. With appropriate attention to the transport logic, self-shielding can be well simulated even in the absence of detailed knowledge of the energy-dependence of the cross section. The current data distribution incorporates probability-table data into the cross-section tables of 72 isotopes among 21 elements from Z=40 to Z=98.

FIGURE 2 place holder

FIGURE 2. Total cross section for ^{235}U from ENDF/B-V and from ENDF/B-VI showing the detailed representation of the resonance region only up to 0.08 keV for the earlier evaluation (92235.50c) and up to 2.25 keV for the later (92235.69c). Neither evaluation provides a complete representation up to the true end of the resonance region (about 25 KeV).

THERMAL ISSUES

Each neutron transport table in the data distribution has been created for a specific temperature. Usually this is room temperature (293.6 K), but for selected isotopes, other temperatures (*e.g.* 20 K, 77 K, 600 K, 3000 K, *etc.*) are provided. For simulations of systems at temperatures other than those provided in the cross-section sets, the results can be affected because of the different thermal velocities of the target nuclei. In MCNP there is a straightforward analytic/stochastic method (the free-gas model) for dealing with this situation, but this method applies only to the elastic scattering channel of the cross section. For problems not dominated by elastic scattering, the temperature dependences can be important. The differences in the resonance region between cross sections evaluated at different temperatures can be quite significant and can have severe effects on the results of the calculation. One really needs cross-section sets evaluated at the correct temperature of the system.

MCNP does not use the ENDF-format files directly. Rather a processing code such as NJOY[10] is used to write the cross-section tables in a format called ACE (A Compact ENDF) with is used directly by the code. It is at this step that a specific temperature is selected. Thus to generate cross sections at a particular temperature not available in the standard distribution, one would expect to have to run NJOY. This has never been an easy matter for the ordinary applications programmer, because NJOY is an extremely complex program with a daunting array of options, and is generally considered something that should be approached only by a specialist in the program. Recently, however, the portion of the logic of NJOY relating to temperature dependence has been isolated in a user-friendly code called DOPPLER[11] and, even more conveniently, has been incorporated into the cross-section librarian called MAKXSF, which is distributed with the MCNP code and data. It is now easy for the user to take an existing cross-section table (or two) and generate a corresponding table at a different temperature. There are two cases. First, for tables in which the resonance region is completely described (or for an application in which the unresolved resonance region is unimportant) one needs only a reference table at a lower temperature than that desired. The MAKXSF code can produce a Doppler-broadened table for the needed temperature. Second, for unresolved-resonance probability tables or for the $S(\alpha,\beta)$ thermal tables to be discussed in the next section, one needs tables evaluated above and below the desired temperature. Then the MAKXSF code can interpolate to produce a table at any temperature between the two reference tables.

THERMAL NEUTRON TRANSPORT TABLES

In the previous section we discussed issues related to thermal motion of target nuclei and associated with Doppler broadening and neutron/nucleus kinematics. There are also more difficult issues affecting low-energy transport, including molecular binding effects, vibrational/rotational levels, lattice spacing, crystal structure, and other solid- and liquid-state properties. The standard ENDF evaluations concentrate on the neutron/nucleus interaction and do not address these matters. Revisiting Figure 1, for example, we see no detail at low energies. In the thermal region, at energies from about 4 eV down to 10^{-5} eV, the cross sections fall into simple $1/v$ form ignoring the complexities of the low-energy regime. In MCNP the best currently-available approach to improving this situation is the use of $S(\alpha,\beta)$ transport tables. These tables are presented as scattering matrices, correlated in scattered energy and angle, and attempting to represent the effects of many of the physical processes that complicate the low-energy neutron transport. When present, they replace the standard cross sections for neutron energies below 4 eV. For applications in which the thermal regime is important, the use of appropriate $S(\alpha,\beta)$ tables can be essential for obtaining accurate results. In the current data distribution there are $S(\alpha,\beta)$ tables available at a variety of relevant temperatures for beryllium metal, beryllium oxide, benzene, ortho and para liquid hydrogen, ortho and para liquid deuterium, graphite, deuterium in heavy water, hydrogen in light water, hydrogen in liquid methane, hydrogen in polyethylene, hydrogen in solid methane, and hydrogen and zirconium in zirconium hydride. Although this collection is a powerful resource for applications that are covered by this list, it is clear that this is a very limited list considering the vast range of applications that can arise in the thermal regime. Obviously this is an area that can benefit greatly from future expansion.

PHOTO-ATOMIC AND ELECTRON TRANSPORT TABLES

MCNP also simulates the coupled photon/electron cascade using methods based on those of the ETRAN[12] codes and of the Integrated TIGER Series[13]. Photo-atomic transport tables provide data describing the four basic photon interaction processes. (1) At photon energies above the threshold ($2mc^2$ for electron mass m), the photon may produce an electron/positron pair. The selection of energies for the two products is based on Bethe-Heitler theory[14], and the angular distribution comes from an adaptation of high-energy theory. Triplet production is not considered separately from pair production. (2) Compton (incoherent) scattering is based on the Klein-Nishina[15] cross section, but is modified by form factors that partially account for the effects of binding energy on the angular distribution[16]. In a recent enhancement, MCNP also takes advantage of data to include the effects of the momentum of bound electrons on the Compton energy distribution. This capability is sometimes confusingly called Compton Doppler broadening, but does not have anything to do with thermal motions of the target atoms, which are not considered for photon or electron transport in MCNP. (3) Thomson (coherent) scattering, arguably the least important of the principal processes, is optionally included in the transport and is also modified by form factors. (4) The photoelectric interaction is the most approximate of the four treatments. MCNP treats only K-shell vacancies and produces at most two fluorescent photons or an Auger electron. The lines that may be selected are restricted to (L3 → K), (L2 → K), (mean M → K), (mean N → K), and (mean upper levels → L). These limitations are somewhat mitigated by the fact that photon/electron transport in MCNP never extends below 1 keV, and is often limited to still higher energies. Nevertheless, the improvement of the treatment of this low-energy regime is a desired future plan for the MCNP/X developers. The upper energy limit for the most recent photo-atomic tables is 100 GeV.

Electron tables, supplemented by analytic models, also support the modeling of the photon/electron cascade. MCNP treats bremsstrahlung as in Version 3 of the Integrated TIGER Series[17], including its effect on stopping powers. Knock-on electrons are sampled from the Møller cross section[18], with angular distributions determined from kinematics. Characteristic X-ray and Auger electron production rely on Kolbenstvedt's cross section[19] and are restricted to the same lines mentioned above for photoelectric events. The electron angular deflection is calculated from the Goudsmit-Saunderson distribution[20], and the electron energy loss straggling is based on Landau's theory[21] with the various extensions described in Ref. 12. The low-energy limit of the MCNP electron tables is 1 keV, as is the case with photo-atomic tables. For historical reasons, the upper energy limit for the electron tables is 1 GeV.

PHOTONUCLEAR TABLES

A recent enhancement of the transport capabilities of MCNP is the addition of code and data to support the simulation of photonuclear reactions at low energies. (Various event-generator models such as the Cascade Exciton Model[22] and Los Alamos Quark-Gluon-String Model[23] deal with photonuclear reactions, but become increasingly uncertain at low energies.) Photonuclear tables contain energy-dependent photon cross sections for nuclear interactions leading to the production of photons, neutrons, protons, deuterons, tritons, helions (^{3}He), and alpha (^{4}He) particles. The tabular data are limited to energies below 150 MeV and address photoabsorption by the excitation of either the giant dipole resonance[24] or a quasi-deuteron nucleon pair[25-27]. Production data including energy and angular distributions are given. In contrast to photo-atomic tables, which are provided for elements and make no distinction among isotopes, the photonuclear tables are isotope-specific. The initial release[28] of photonuclear tables for MCNP/X contained only 13 isotopes: ^{2}H, ^{12}C, ^{16}O, ^{27}Al, ^{28}Si, ^{40}Ca, ^{56}Fe, ^{63}Cu, ^{181}Ta, ^{184}W, ^{206}Pb, ^{207}Pb, and ^{208}Pb. This is an area which will be greatly aided by the eventual availability to MCNP/X of the newly released ENDF/B-VII data[29]. That compilation will include a new sub-library with 163 photonuclear evaluations.

PROTON TRANSPORT TABLES

Proton transport tables were developed at Los Alamos in order to support the Accelerator Production of Tritium program, the same program that was a major driving force behind the original development of the MCNPX code itself. These tables include total, nuclear elastic plus interference, and inelastic cross sections; production cross sections for photons, neutrons, protons, deuterons, tritons, hellions, alphas, and heavy recoils; double-differential (energy and angle) production spectra for neutrons, protons, deuterons, tritons, hellions, and alphas; and angle-integrated emission spectra for photons and heavy recoils. Like the photonuclear tables, proton tables provide data up to 150 MeV. These tables are intended to describe nuclear reactions only: energy loss and angular deflection caused by collisional multiple scattering are to be modeled by other methods. Traditionally in MCNPX, these processes were simulated using the Vavilov[30] model and a Gaussian approximation[31] described by Rossi. Recently we have developed and implemented a new multiple scattering model[32] that takes into account projectile and nuclear target form factors, and provides a coupled sampling of both collisional energy loss and angular deflection.

The initial release[33] of proton transport tables for MCNPX included 42 isotopes ranging from ^{1}H to ^{209}Bi. The release if ENDF/B-VII[29] will expand this list somewhat, adding six more proton tables and introducing five tables for deuteron projectiles, three for tritons, and two for helions. The new projectile types will present a welcome challenge to MCNP/X developers to generalize the code, which currently assumes that only neutrons, photons, electrons, and protons make use of transport tables.

SUMMARY

We have presented a basic introduction to the capabilities of the MCNP and MCNPX transport codes in the low-energy regime, with particular attention to the use of transport data tables. These codes offer powerful and accurate methods for the simulation of particle transport, especially for applications in which the details of all energy ranges are important.

REFERENCES

1. X-5 Monte Carlo Team, *MCNP — A General Monte Carlo N-Particle Transport Code, Version 5, Volume I: Overview and Theory*, Los Alamos National Laboratory report LA-UR-03-1987 (April 24, 2003).
2. H. G. Hughes, K. J. Adams, M. B. Chadwick, J. C. Comly, S. C. Frankle, J. S. Hendricks, R. C. Little, R. E. Prael, L. S. Waters, P. G. Young, "MCNPX — The LAHET/MCNP Code Merger," in Proceedings of the Third Workshop on Simulating Accelerator Radiation Environments (SARE3), May 7-9, 1997, Tsukuba, Japan (KEK Proceedings 97-5, June 1997) pp. 44-51.

3. H. Grady Hughes, Forrest B. Brown, Jeffrey S. Bull, John T. Goorley, Robert C. Little, Lon-Chang Liu, Stepan G. Mashnik, Richard E. Prael, Elizabeth C. Selcow, Arnold J. Sierk, Jeremy E. Sweezy, John D. Zumbro, Nikolai V. Mokhov, Sergei I. Striganov, Konstantin K. Gudima, "MCNP5 for Proton Radiography," in The Monte Carlo Method: Versatility Unbounded in a Dynamic Computing World, proceedings of Monte Carlo 2005, Chattanooga, Tennessee, April 17-21, 2005. On CD-ROM, American Nuclear Society, LaGrange Park, IL (2005).
4. V. McLane, C. L. Dunford, P. F. Rose, ed., "ENDF-102: Data Formats and Procedures for the Evaluated Nuclear Data File, ENDF-6," Brookhaven National Laboratory report BNL-NCS-44945, revised (1995) (available URL: http://www.nndc.bnl.gov/).
5. R. J. Howerton, D. E. Cullen, R. C. Haight, M. H. MacGregor, S. T. Perkins, E. F. Plechaty, "The LLL Evaluated Nuclear Data Library (ENDL): Evaluation Techniques, Reaction Index, and Descriptions of Individual Reactions," Lawrence Livermore Scientific Laboratory report UCRL-50400, Vol. 15, Part A (September 1975).
6. J. E. Morel, L. J. Lorence, Jr., R. P. Kensek, J. A. Halbleib, D. O. Sloan, "A Hybrid Multigroup/Continuous-Energy Monte Carlo Method for Solving the Boltzmann-Fokker-Planck Equation," *Nucl. Sci. Eng.*, **124**, p.369-389 (1996).
7. L. J. Lorence, Jr., J. E. Morel, G. D. Valdez, "Physics Guide to CEPXS: A Multigroup Coupled Electron-Photon Cross-Section Generating Code, Version 1.0," Sandia National Laboratory report SAND89-1685 (1989).
8. M. A. Gardner, R. J. Howerton, "ACTL: Evaluated Neutron Activation Cross-Section Library — Evaluation Techniques and Reaction Index," Lawrence Livermore National Laboratory report UCRL-50400, Vol. 18 (October 1978).
9. L. L. Carter, R. C. Little, J. S. Hendricks, R. E. MacFarlane, "New Probability Table Treatment in MCNP for Unresolved Resonances," *1998 ANS Radiation Protection and Shielding Division Topical Conference, April 19-23, 1998, Nashville, TN*, Vol. II, p. 341-347.
10. R. E. MacFarlane, D. W. Muir, "The NJOY Nuclear Data Processing System, Version 91," Los Alamos National Laboratory report LA-12740-M (1994).
11. R. E. MacFarlane, P. Talou, "DOPPLER: A Utility Code for Preparing Customized Temperature-Dependent Data Libraries for the MCNP Monte Carlo Transport Code," Los Alamos National Laboratory internal report (Oct. 3, 2003).
12. Stephen M. Seltzer, "An Overview of ETRAN Monte Carlo Methods," in *Monte Carlo Transport of Electrons and Photons*, edited by Theodore M. Jenkins, Walter R. Nelson, and Alessandro Rindi, p. 153 (Plenum Press, New York, 1988).
13. J. Halbleib, "Structure and Operation of the ITS Code System," *ibid*, p. 249.
14. H. A. Bethe, J. Ashkin, "Passage of Radiations through Matter," in *Experimental Nuclear Physics, Vol. I*, edited by E. Segre (John Wiley, New York, 1953) p. 166.
15. O. Klein, Y. Nishina, "Über die Streuung vol Strahlung durch freie Elektronen nach der neuen relativistischen Quantendynamik von Dirac," *Z. Phys.* **52** (1929) 853.
16. J. F. Williamson, F. C. Diebel, R. L. Morin, "The Significance of Electron-Binding Corrections in Monte Carlo Photon Transport Calculations," *Phys. Med. Biol.* **29** (1984) 1063.
17. S. M. Seltzer, "Cross Sections for Bremsstrahlung Production and Electron-Impact Ionization," in *Monte Carlo Transport of Electrons and Photons*, edited by Theodore M. Jenkins, Walter R. Nelson, and Alessandro Rindi, p.81.
18. C. Møller, "Zur Theorie des Durchgang schneller Elektronen durch Materie," *Ann. Physik.* **14** (1932) 568.
19. H. Kolbenstvedt, "Simple Theory for K-Ionization by Relativistic Electrons," *J. Appl. Phys.* **38** (1967) 4785.
20. S. Goudsmit, J. L. Saunderson, "Multiple Scattering of Electrons," *Phys. Rev.* **57** (1940) 24.
21. L. Landau, "On the Energy Loss of Fast Particles by Ionization," *J. Phys. (USSR)* **8** (1944) 201.
22. Gudima, K. K., Mashnik, S. G., and Toneev, V. D. *Cascade-exciton model of nuclear reactions*, Nucl. Phys. **A401**, 329 (1983).
23. Gudima, K. K., Mashnik, S. G., and Sierk, A. J. *User Manual for the Code LAQGSM*, Los Alamos National Laboratory report LA-UR-01-6804 (2001).
24. A. Bohr, B. R. Mottelson, *Nuclear Structure*, 2nd Edition (World Scientific: Singapore 1998).
25. J. S. Levinger, "Neutron Production by Complete Absorption of High-Energy Photons," *Nucleonics* **6** #5 (1950) 64.
26. J. S. Levinger, "The High-Energy Nuclear Photoeffect," *Phys. Rev.* **84** #1 (1951) 43.
27. M. B. Chadwick, P. Oblozinsky, P. E. Hodgson, G. Reffo, "Pauli-Blocking in the Quasideuteron Model of Photoabsorption, *Phys. Rev. C* **44** #2 (1991) 814.
28. M. C. White, "Release of the LA150U Photonuclear Data Library," Los Alamos National Laboratory memorandum X-5:MCW-00-87(U), July 26, 2000, revised March 21, 2001.
29. M. B. Chadwick, P. Oblozinsky, M. Herman, *et al.*, "ENDF/B-VII.0: Next Generation Evaluated Nuclear Data Library for Nuclear Science and Technology," *Nuclear Data Sheets* **107** #12 (2006) 2931.
30. P. V. Vavilov, "Ionization Losses of High-Energy Heavy Particles," *Soviet Physics JETP* **5** (4) (1957) 749.
31. B. Rossi, *High-Energy Particles*, Prentice-Hall, Incorporated, New York 1952.

32. S. Striganov "On Theory and Simulation of Multiple Coulomb Scattering of Heavy Particles," in *Proceedings of the ICRS 10/RPS 2004*, Madeira, Portugal, 9-14 May 2004.
33. M. B. Chadwick, P. G. Young, S. Chiba, S. Frankle, G. M. Hale, H. G. Hughes, A. J. Koning, R. C. Little, R. E. MacFarlane, R. E. Prael, L. S. Waters, "Cross Sections Evaluations to 150 MeV for Accelerator-Driven Systems Implementation in MCNPX," *Nucl. Sci. Eng.* **131** (1999) 293.

Figure 1

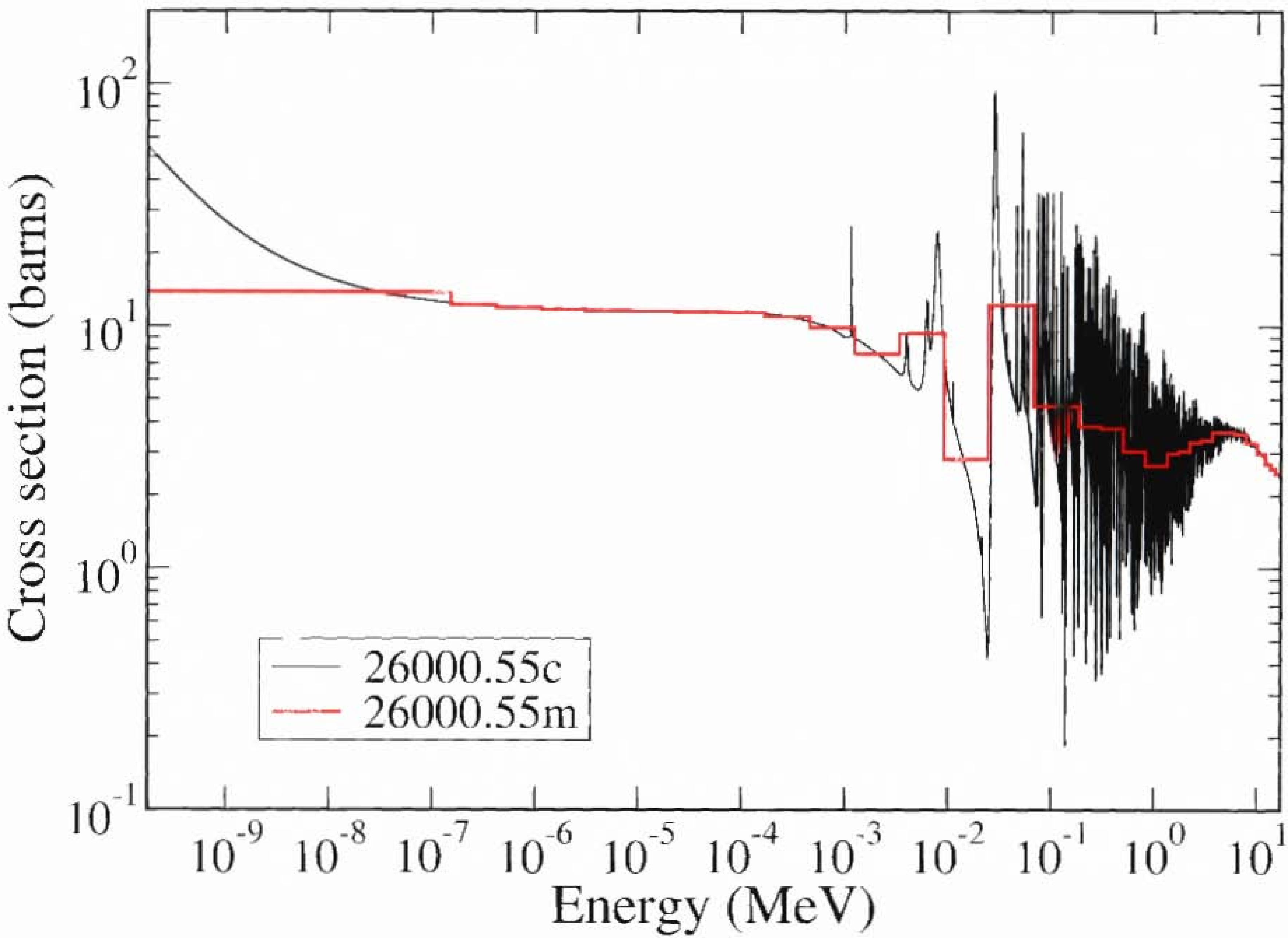

Cross section (barns)
10^{2}
10^{1}
10^{0}
10^{-1}
10^{-9} 10^{-8} 10^{-7} 10^{-6} 10^{-5} 10^{-4} 10^{-3} 10^{-2} 10^{-1} 10^{0} 10^{1}
Energy (MeV)
26000.55c
26000.55m

Figure 2

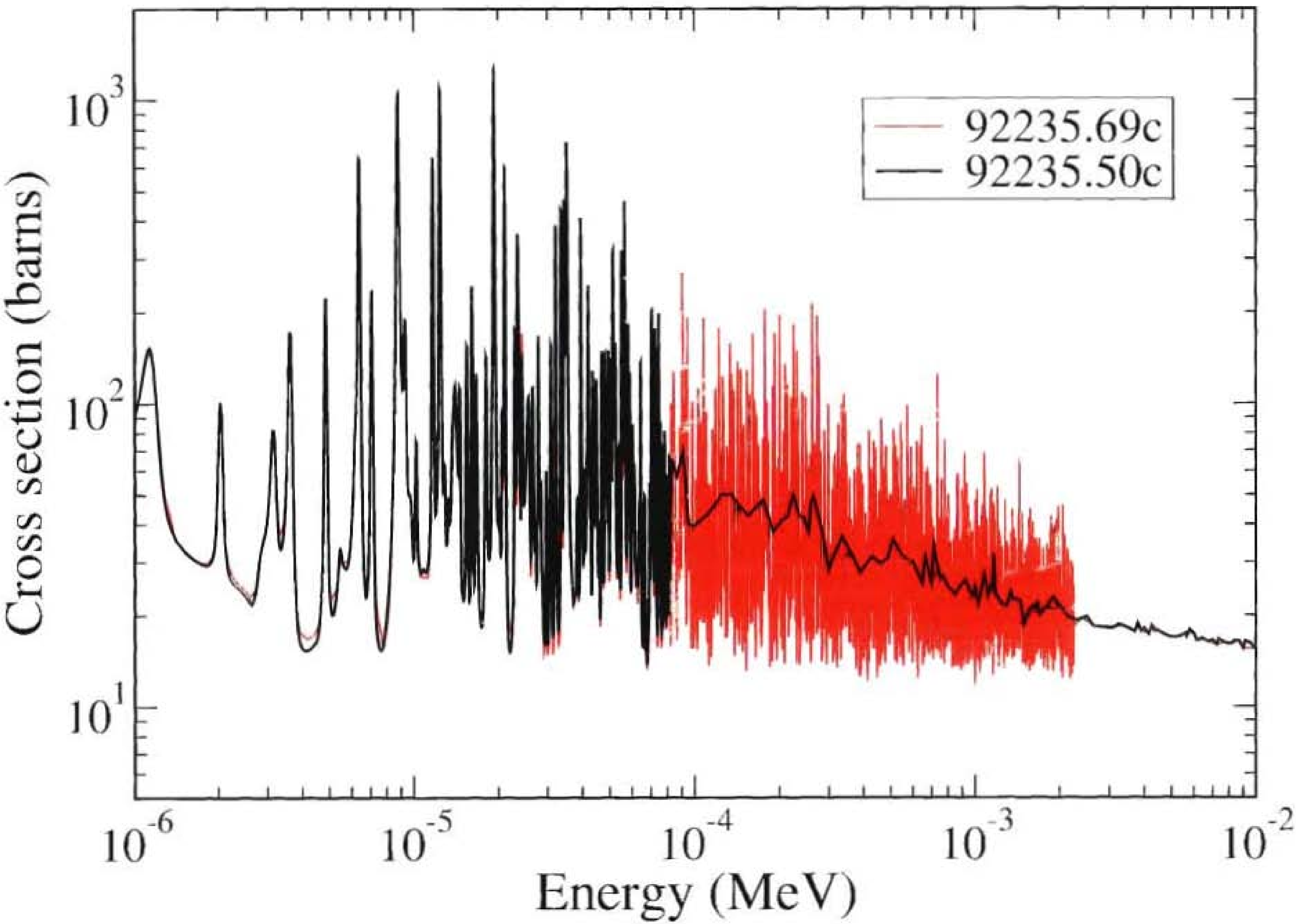

92235.69c
92235.50c
Cross section (barns)
10^3
10^2
10^1
10^{-6}
10^{-5}
10^{-4}
10^{-3}
10^{-2}
Energy (MeV)